minerals

MDPI

Article

Co-Bioleaching of Chalcopyrite and Silver-Bearing Bornite in a Mixed Moderately Thermophilic Culture

Congren Yang [1,2], Fen Jiao [1] and Wenqing Qin [1,*]

1 School of Minerals Processing and Bioengineering, Central South University, Changsha 410083, China; yangcongren@csu.edu.cn (C.Y.); jfen0601@126.com (F.J.)
2 School of Environment, Tsinghua University, Beijing 100084, China
* Correspondence: qinwenqing369@126.com; Tel.: +86-731-8883-0884

Received: 22 October 2017; Accepted: 20 December 2017; Published: 26 December 2017

Abstract: Chalcopyrite and bornite are two important copper minerals, and they often coexist. In this study, the co-bioleaching of chalcopyrite and silver-bearing bornite by mixed moderately thermophilic culture at 50 °C was investigated. The bioleaching results show that the extraction percentage of Cu for co-bioleaching of chalcopyrite (Ccp) and silver-bearing bornite (Bn) (Ccp/Bn = 3:1) was 94.6%. Compared to bioleaching of chalcopyrite or silver-bearing bornite alone, the Cu extraction percentage was greatly enhanced when they were bioleached together. The leaching residues were characterized by X-ray diffraction (XRD) and X-ray photoelectron spectroscopy (XPS). Silver-bearing bornite dissolved preferentially compared to chalcopyrite, due to galvanic interactions. Simultaneously, Ag^+ was released from the silver-bearing bornite into solution. Ag_2S formed on the surface because Cu and Fe in the chalcopyrite were replaced by Ag^+, accelerating chalcopyrite dissolution and enrichment of Ag on the surface of the chalcopyrite.

Keywords: co-bioleaching; chalcopyrite; bornite; galvanic interaction; silver-catalyzed

1. Introduction

Chalcopyrite ($CuFeS_2$) is a primary copper resource worldwide [1,2], and hydrometallurgy of chalcopyrite has been attracting more and more research attention [3–6]. Chalcopyrite is difficult to be leached, though, owing to the passivation of the mineral surface [7–10], which contains S_2^{2-} [7,11], S_n^{2-} [7,12], $Cu_{1-x}Fe_{1-y}S_{2-z}$ [13,14], Cu_5FeS_4 [13], CuS [13], CuS_2 [15], S^0 [11], and jarosite [11,16], all considered passivation composites. However, Crundwell et al. [17] argued that the rate of chalcopyrite dissolution is intrinsically slow due to its semiconducting properties, and is not limited by passivation film. Several studies have been undertaken to improve chalcopyrite leaching [18–21]. Redox potential, or the ratio of Fe^{3+}/Fe^{2+}, is considered to play a key role in chalcopyrite leaching [8,9,22–24]. Hiroyoshi et al. [25] found that the leaching of chalcopyrite can be accelerated by the addition of Fe^{2+} and Cu^{2+}. The leaching efficiency of chalcopyrite can also be improved by the addition of pyrite, because of its galvanic interaction [26,27], and also the addition of silver ions or silver-bearing materials greatly enhances the dissolution of chalcopyrite [28–33]; several different mechanisms have been proposed for silver-catalyzed chalcopyrite leaching [34–38].

A number of studies have been conducted on the bioleaching of bornite [39–42] because bornite (Cu_5FeS_4) is another important Cu-Fe-S mineral [1]. The bioleaching of bornite by *Acidithiobacillus ferrooxidans* was evaluated in oxygen uptake and shake flask experiments. Covellite was detected as a secondary phase [43], and cell action on the surface of the bornite accelerated the leaching rate via both direct and indirect mechanisms [44]. Recently, the combined effects of chalcopyrite and bornite during bioleaching have been investigated, and it was found that the bioleaching of chalcopyrite was enhanced in the presence of bornite [41,45,46].

Chalcopyrite and bornite are two important Cu-Fe-S minerals, and they often coexist [47–49]. The objective of this research was to investigate the co-bioleaching of chalcopyrite and silver-bearing bornite using a mixed moderately thermophilic culture at 50 °C. The leaching residues were characterized by X-ray diffraction (XRD) and X-ray photoelectron spectroscopy (XPS).

2. Materials and Methods

2.1. Mineral Samples

The chalcopyrite used in this study was obtained from Tonglvshan Mine, Daye, China. The bornite samples were purchased from GaoWanTong fossil specimen museum, Guilin, China. High-quality natural mineral samples were splintered into small fragments using a geological hammer, and then dry ground with porcelain ball milling. The particle size of the samples used for the bioleaching experiments was less than −0.074 mm. Chemical analysis of the samples showed that the chalcopyrite sample consisted of 33.91% Cu, 30.62% Fe, 32.90% S, 0.039% Pb, 0.018% Zn and 6.91 g/t Ag; and the bornite samples, of 62.38% Cu, 10.55% Fe, 22.60% S, 0.500% Pb, 0.048% Zn and 4635.48 g/t Ag. Aside from the special notes, all of the percentages (%) in this paper refer to weight percentage (wt %).

2.2. Bioleaching Experiments

The mixed moderately thermophilic culture consisted of *Sulfobacillus thermosulfidooxidans*, together with a small amount of *Acidithiobacillus caldus* and *Ferroplasma* sp; this culture was an enrichment from a leaching solution sample at 50 °C, and was obtained from Inner Mongolia, China [7]. In each experiment, 2 g of sample was added into 250 mL flasks containing 100 mL of medium (components: 3.0 g/L $(NH_4)_2SO_4$, 0.5 g/L K_2HPO_4, 0.5 g/L $MgSO_4{\cdot}7H_2O$, 0.1 g/L KCl, 0.01 g/L $Ca(NO_3)_2$, and 0.02% yeast extract, with a pH of 1.6). The experimental sets are presented in Table 1. The initial concentration of cells was 1.0×10^7 cells/mL. The flasks were placed in an orbital shaker at 160 rpm and 50 °C. The solution pH was adjusted periodically to 1.6 with diluted sulfuric acid. In addition, 1.0 mL of leaching solution was sampled and analyzed for Cu and Fe using inductively coupled plasma-atomic emission spectrometer (ICP−AES) (PS−6, Baird, Bedford, MA, USA). The sample volume was replaced with an equal volume of medium. Water lost to evaporation was supplemented periodically by adding distilled water until the mass of the flask equaled its initial mass.

Table 1. Leaching experiment sets.

No.	$CuFeS_2$ (g)	Cu_5FeS_4 (g)	Condition
1	2	0	Sterile control
2	2	0	Bioleaching
3	0	2	Sterile control
4	0	2	Bioleaching
5	0.5	1.5	Bioleaching
6	1.0	1.0	Bioleaching
7	1.5	0.5	Bioleaching

2.3. Electrochemical Test

The electrodes were prepared from high-quality natural chalcopyrite and bornite. The effective area of the electrode exposed to the solution was 1 cm^2. Before each electrochemical test, the surface of the electrode was polished with 600-grit and 2500-grit metallographic abrasive papers, sequentially, and then rinsed with deionized water. Electrochemical tests were performed using a conventional three-electrode electrolytic cell: a counter electrode (graphite rod), a reference electrode (saturated Ag/AgCl electrode), and a working electrode (chalcopyrite or bornite electrode). The electrolyte solution consisted of 3.0 g/L $(NH_4)_2SO_4$, 0.5 g/L K_2HPO_4, 0.5 g/L $MgSO_4{\cdot}7H_2O$, 0.1 g/L KCl, and 0.01 g/L $Ca(NO_3)_2$, pH 1.6. The scan rate of the Tafel polarization was 0.5 mV/s. All tests were conducted at 50 °C.

2.4. Analytical Techniques

The solution pH was measured with a pH meter (BPP-922, BELL Analytical Instruments (DaLian) Co., Ltd., Dalian, China) and the solution potentials were measured with a Pt electrode with reference to a saturated Ag/AgCl electrode. The leaching residues were filtered and rinsed with dilute sulfuric acid (pH 1.6) at room temperature and atmosphere, and then the samples were transferred into a vacuum box, and dried at 40 °C; afterwards, all of these properly dried samples were used for analysis with XRD (Advance D8, Bruker AXS, Karlsruhe, Germany) and XPS (ESCALAB 250Xi, Thermo Fisher Scientific, Waltham, MA, USA). XPS was conducted with a monochromatic Al excitation (1486.6 eV) operating at 200 W, and the chamber pressure was 1×10^{-9} mbar. High-resolution spectra were collected using a pass energy of 20 eV and an energy step of 0.1 eV. Binding energy calibration was based on C 1s at 284.6 eV. A summed Gaussian (70%)–Lorentzian (30%) function was used for peaks fitted to the high-resolution spectra.

3. Results

3.1. Leaching Characteristics

The leaching characteristics of the minerals, in terms of changes in the extraction percentages of Cu and Fe, pH and redox potentials, by sterile controls and microorganisms, are shown in Figure 1.

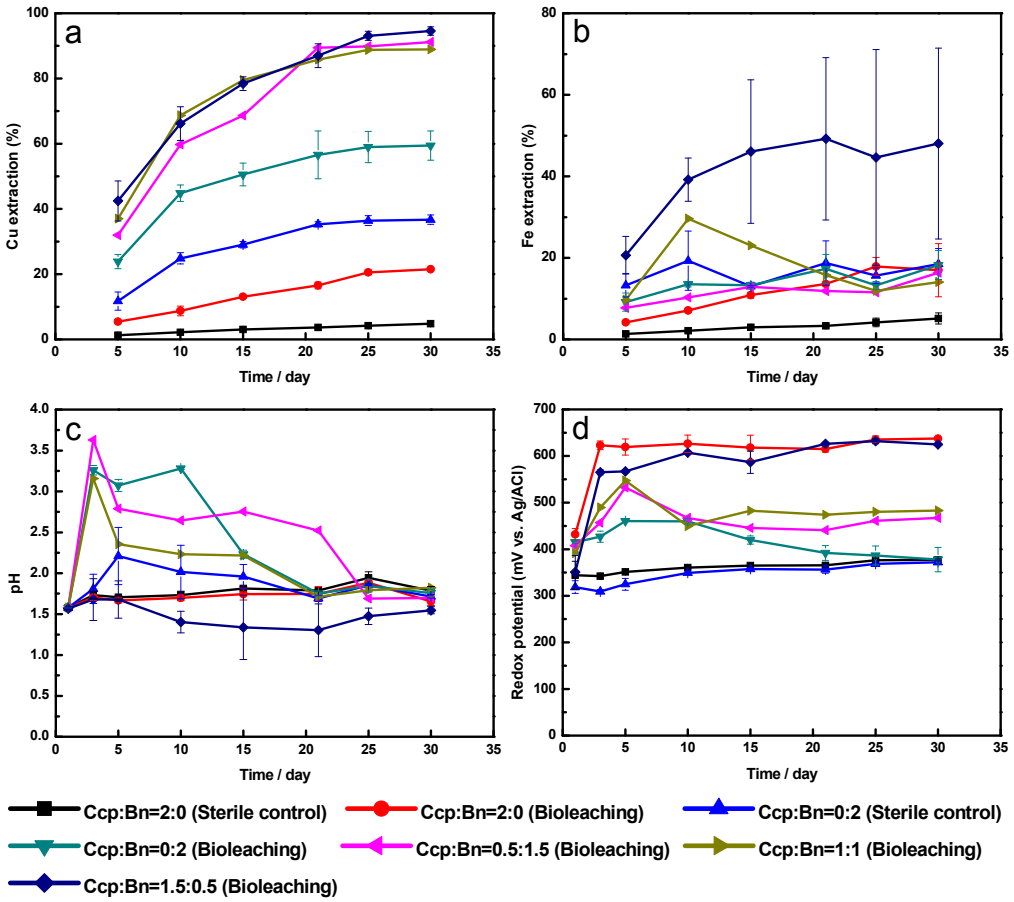

Figure 1. Copper extraction (**a**); iron extraction (**b**); pH (**c**) and redox potential (**d**) in leach liquors during the leaching process.

Under the sterile control, 4.8% of the Cu and 5.1% of the Fe were leached from the chalcopyrite after 30 days (Figure 1a,b), and compared to chemical leaching, the extraction percentages of Cu and Fe for bioleaching of chalcopyrite were 21.5% and 17.0%, respectively. Simultaneously, the Fe extraction

percentage decreased owing to the precipitation of Fe^{3+} as jarosite after 24 days of bioleaching [7,50]. The pH of the solution changed slightly because only a small amount of chalcopyrite was leached either by chemically or microorganisms (Figure 1c). During the bioleaching of chalcopyrite, Fe^{2+} in the solution was oxidized to Fe^{3+} by ferrous oxidizing microbials, and thus redox potentials rose and stabilized at about 630 mV, while the redox potentials of chemical leaching stabilized at about 370 mV (Figure 1d).

The extraction percentages of Cu and Fe for the chemical leaching of bornite after 30 days were 36.7% and 18.5%, respectively, whereas 59.4% of Cu and 18.2% of Fe were bioleached from the bornite. Figure 1c shows that a large amount of H^+ was consumed during both chemical and bio-leaching of bornite. In the first 10 days of bornite bioleaching, the Fe^{2+} was oxidized into Fe^{3+} by ferrous oxidizing microbials, resulting in a redox potential increase to 460 mV. The potential slowly decreased from 460 to 380 mV over the following 20 days because the rate of Fe^{2+} oxidation to Fe^{3+} by the microorganisms was less than the consumption rate of Fe^{3+} via bornite oxidation (Figure 1d). In contrast, the potentials increased slowly and reached 370 mV after 30 days of leaching in the sterile control.

Compared to bioleaching of chalcopyrite (Ccp) or bornite (Bn) alone, the Cu extraction percentage was greatly enhanced in co-bioleaching (Figure 1a). When the ratio of Ccp/Bn was 1:3, the extraction percentages of Cu and Fe for co-bioleaching of chalcopyrite and bornite were 91.1% and 16.4%, respectively; and when the ratio of Ccp/Bn was 1:1, 89.0% of the Cu and 11.9% of the Fe were synergistically bioleached after 30 days. Interestingly, when the ratio of Ccp/Bn was 3:1, the extraction percentage of the Cu and Fe for co-bioleaching of chalcopyrite and bornite were 94.6% and 48.0%, respectively.

A large amount of H^+ was consumed during the co-bioleaching of chalcopyrite and bornite (Figure 1c). When the ratio of Ccp/Bn was 1:3 or 1:1, the change in redox potentials was similar to that when leaching bornite alone. In the first five days of co-bioleaching chalcopyrite and bornite, the redox potentials went up to about 540 mV, and then the potential slowly decreased and finally stabilized in the range of 450 to 480 mV. However, the redox potentials were still higher than those from leaching bornite alone (Figure 1d). When the ratio of Ccp/Bn was 3:1, the change in redox potentials was similar to that of leaching chalcopyrite alone. The redox potential increased with time and finally reached 630 mV (Figure 1d).

In summary, 21.5% of Cu was bioleached from the chalcopyrite; compared to bioleaching of chalcopyrite, bornite was more easily bioleached, but 40.6% of the Cu was still locked in the residues. When chalcopyrite and silver-bearing bornite were co-leached in a mixed moderately thermophilic culture, both Cu extraction percentages were greatly enhanced.

3.2. Characterization of the Leaching Residues

In order to better understand the co-bioleaching of chalcopyrite and bornite (when the ratio of Ccp/Bn was 3:1) in a mixed moderately thermophilic culture, the leaching residues were characterized by XRD and XPS.

As shown in Figure 2, the XRD patterns of co-bioleaching chalcopyrite and bornite (when the ratio of Ccp/Bn was 3:1) show that only the characteristic peaks of chalcopyrite were detected after 5 and 10 days of bioleaching (Figure 2D,E). Simultaneously, the mineralogical analysis of the leaching residues shows that 81% of the bornite and 15% of the chalcopyrite were bioleached after 5 days. Thus, the bornite preferentially dissolved. When the mixed sample was bioleached for 15 days, the main composition of the leaching product was still chalcopyrite, together with low-intensity peaks of jarosite (Figure 2F). Jarosite and elemental sulfur were detected after 30 days of bioleaching, and, at the same time, low-intensity peaks of chalcopyrite were detected (Figure 2G).

The chalcopyrite, bornite, and leaching residues were also analyzed using XPS. The survey (full range) XPS spectra of the samples are provided in Figure 3. Prior to the bioleaching of chalcopyrite, C, O, Cu, Fe and S peaks were identified (Figure 3A). For the bornite, in addition to C, O, Cu, Fe, and S peaks, a low-intensity Ag peak was also detected (Figure 3B). The peak intensity of Cu 2p decreased

with leaching time and eventually disappeared. A low-intensity silver peak was detected between 5 and 23 days (Figure 3C–F), but disappeared after 30 days of bioleaching (Figure 3G). A low-intensity nitrogen peak was detected throughout the bioleaching process; this could have originated from ammoniojarosite (Figure 3C–G). The changes in atomic percentages on the surface of residues during the bioleaching process are shown in Figure 3H.

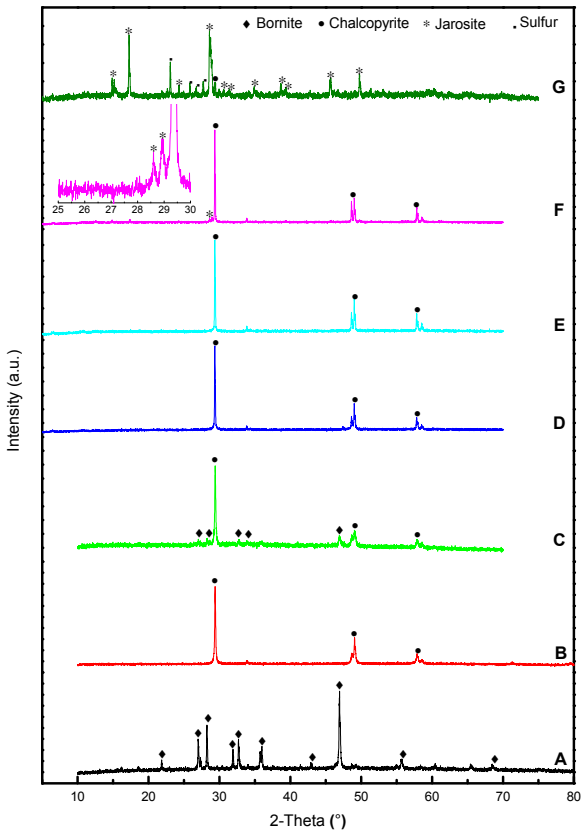

Figure 2. X-ray diffraction (XRD) patterns of co-bioleaching chalcopyrite and bornite (ratio of Ccp/Bn was 3:1). (**A**) bornite, (**B**) chalcopyrite, (**C**) Ccp/Bn = 3:1, (**D**) 5 days, (**E**) 10 days, (**F**) 15 days, (**G**) 30 days.

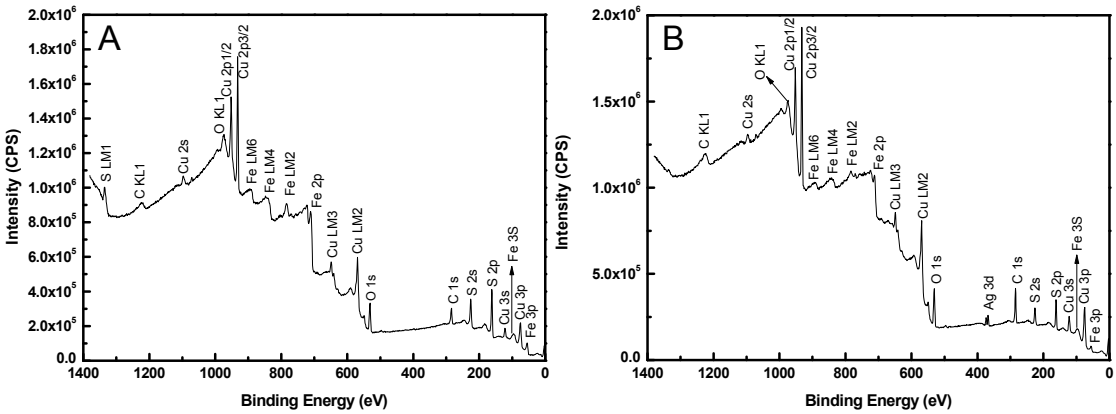

Figure 3. *Cont.*

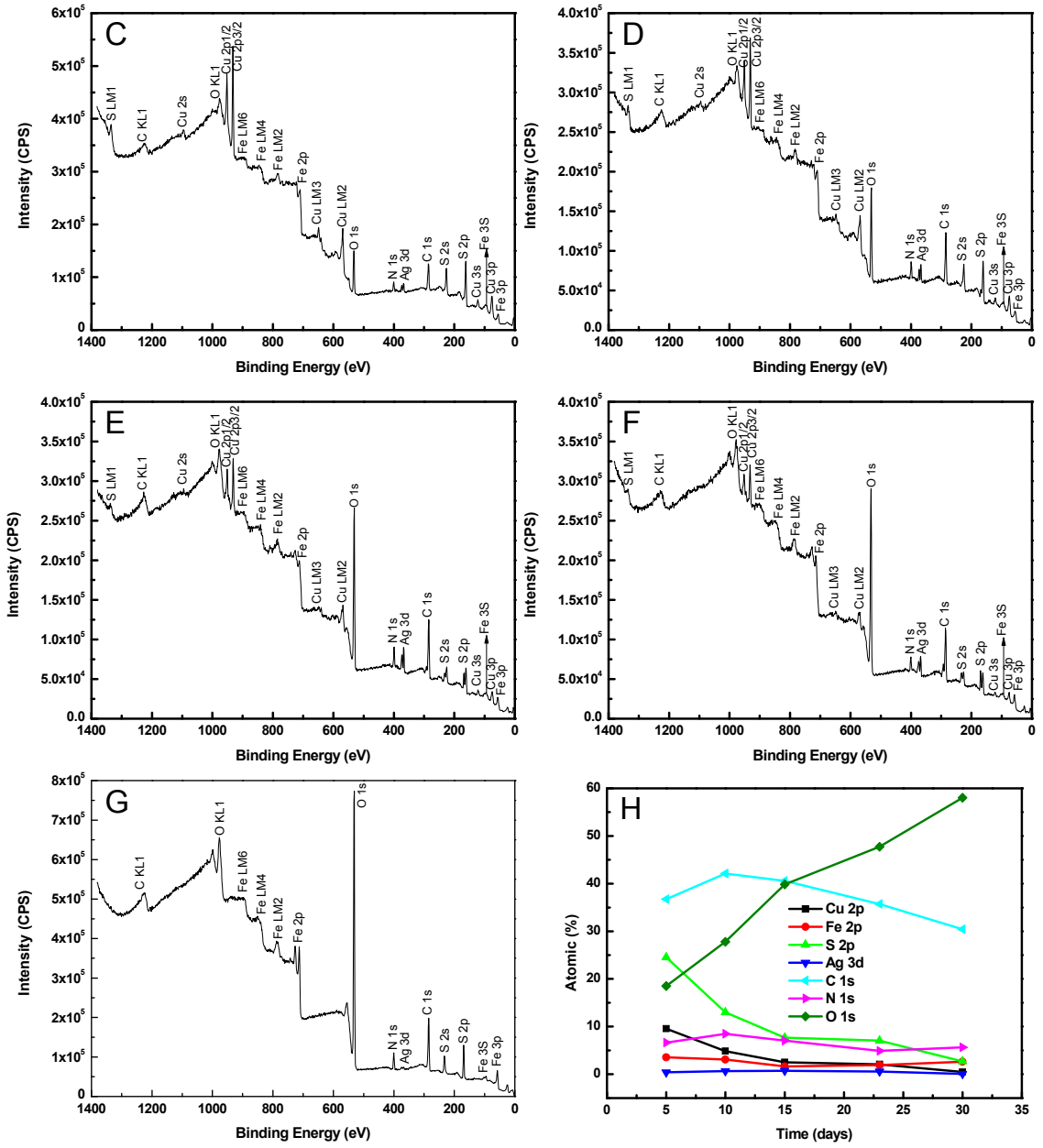

Figure 3. Survey (full range) X-ray photoelectron spectroscopy (XPS) spectra of co-bioleaching of chalcopyrite and bornite (ratio of Ccp/Bn was 3:1). (**A**) chalcopyrite; (**B**) bornite; (**C**) 5 days; (**D**) 10 days; (**E**) 15 days; (**F**) 23 days; (**G**) 30 days. H-Change in atomic percentages on the surface of residues during the bioleaching process. Data source: survey (full range) XPS spectrum.

High-resolution spectra of Cu 2p for bornite, chalcopyrite, and leaching residues are shown in Figure 4. It is well established in literature that the high binding energy (in the range of 933.0 to 933.8 eV) and the presence of a satellite peaks (around 942 eV) are two main XPS characteristics of Cu(II), while a lower binding energy (in the range of 931.8 to 933.1 eV) and the absence of satellite peaks are characteristics of Cu(I) and metal Cu [14,51–53]. From Figure 4, it can be seen that the oxidation state for Cu after bioleaching was still +1. Although low-intensity peaks of chalcopyrite were detected by XRD after 30 days of bioleaching, no Cu peak was detected by XPS. This may be because the chalcopyrite was covered by jarosite and elemental sulfur (Figure 2F).

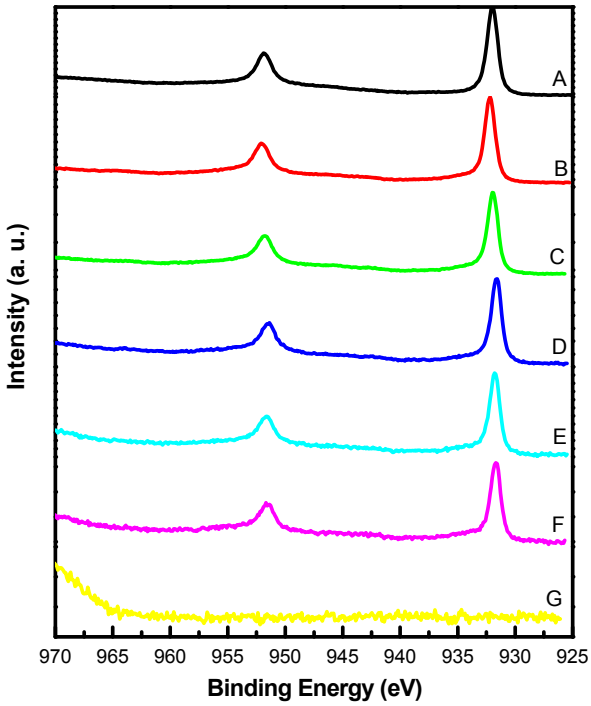

Figure 4. Cu 2p peaks of co-bioleaching chalcopyrite and bornite (ratio of Ccp/Bn was 3:1). (**A**) bornite, (**B**) chalcopyrite, (**C**) 5 days, (**D**) 10 days, (**E**) 15 days, (**F**) 23 days, (**G**) 30 days.

The copper Auger spectra (Cu LMM) excited with X-rays and the atomic percentages of Cu 2p and Ag 3d on the surface of bioleaching residues are shown in Figure 5. It was very interesting that the Cu LMM, Ag $3p_{3/2}$ peak was detected at about 572.5 eV [54] (Figure 5C–F), this was in agreement with the survey XPS spectra (Figure 3C–F). Figure 5C–F show that the peak area ratio of Ag/Cu increased as leaching time increased from 5 to 23 days. Simultaneously, the ratio of Ag_{3d}/Cu_{2p} also increased with leaching time (Figure 5H). These results indicated that silver was enriched on the surface of chalcopyrite and/or bornite. The Ag $3p_{3/2}$ peak disappeared after 30 days of bioleaching (Figure 5G), indicating that silver compounds had been leached and/or covered by jarosite.

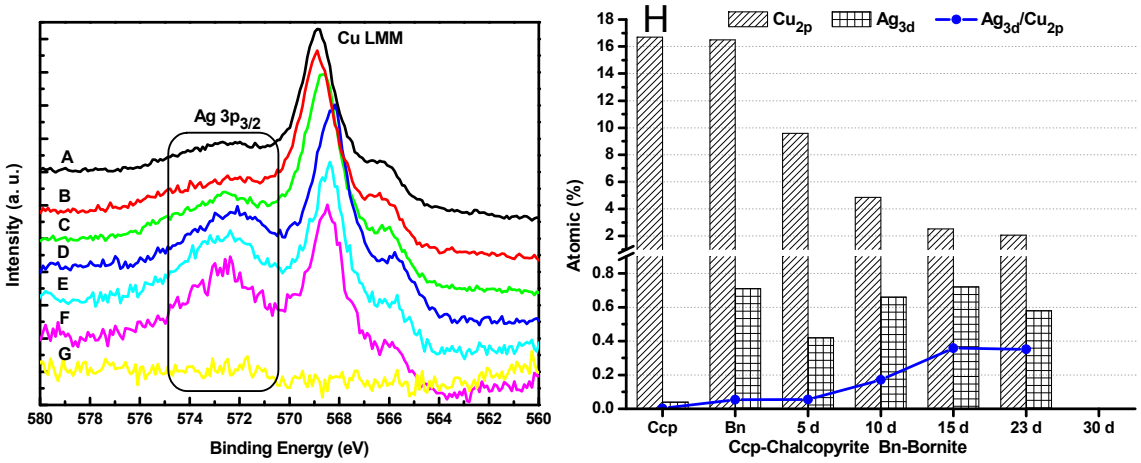

Figure 5. Copper Auger spectra (Cu LMM) peaks of co-bioleaching chalcopyrite and bornite (ratio of Ccp/Bn was 3:1). (**A**) bornite, (**B**) chalcopyrite, (**C**) 5 days, (**D**) 10 days, (**E**) 15 days, (**F**) 23 days, (**G**) 30 days. (**H**) Atomic percentage of Cu 2p and Ag 3d on the surface of bioleaching residues. Data source: survey (full range) XPS spectra.

The high-resolution spectra of S 2p for bornite, chalcopyrite and leaching residues are shown in Figure 6, and the fitted photoelectron spectra of S 2p peaks of Figure 6 are presented in Table 2. In order to obtain the data in Figure 6H, it was assumed that the percentages of S^{2-}, S_2^{2-}, S_n^{2-}, S^0, and SO_4^{2-} were directly proportional to the area under the S 2p peak presented in Figure 6C–G.

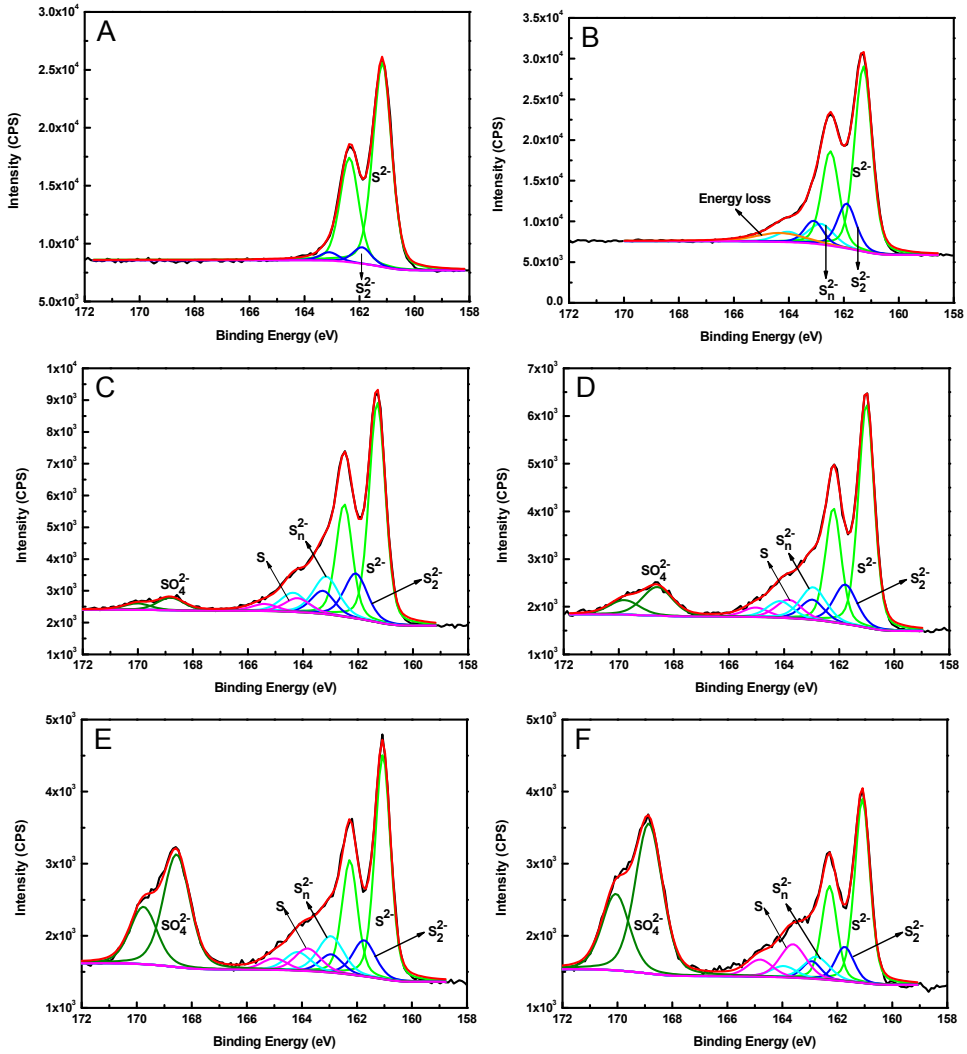

Figure 6. *Cont.*

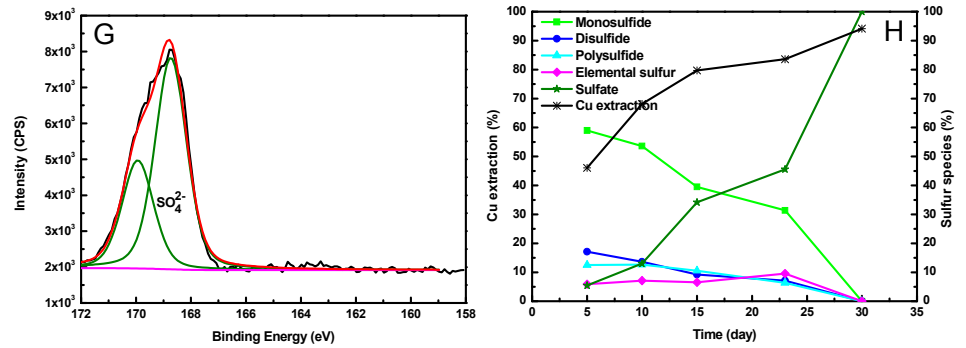

Figure 6. S 2p peaks of co-bioleaching chalcopyrite and bornite (ratio of Ccp/Bn was 3:1). (**A**) bornite; (**B**) chalcopyrite; (**C**) 5 days; (**D**) 10 days; (**E**) 15 days; (**F**) 23 days; (**G**) 30 days; (**H**) Cu extraction and sulfur species on the residue surface.

Table 2. Binding energy values for X-ray photoelectron spectroscopy (XPS) spectra of S $2p_{3/2}$ peaks (eV).

Condition	S^{2-}	S_2^{2-}	S_n^{2-}	S^0	SO_4^{2-}
Cu_5FeS_4	161.2	161.9			
$CuFeS_2$	161.3	161.9	162.8		
5 days	161.3	162.1	163.2	164.2	168.8
10 days	161.0	161.8	162.9	163.8	168.6
15 days	161.1	161.7	163.0	163.8	168.6
23 days	161.1	161.7	162.8	163.6	168.9
30 days					168.7
Ag_2S [#]	160.8				

[#] Data cited from Kaushik [55].

As can be seen from Figure 6C–G, except for the S^{2-} that originated from chalcopyrite, the S_2^{2-}, S_n^{2-}, S^0, and SO_4^{2-} were detected on surface leaching residues during the bioleaching time from 5 to 23 days. Furthermore, the percentage of S^{2-}, S_2^{2-}, S_n^{2-}, and S^0 decreased with increasing time from 5 to 23 days, while the percentage of SO_4^{2-} increased with increasing bioleaching time (Figure 6H). Only SO_4^{2-} was detected on the on surface leaching residues after 30 days of bioleaching. This result is not consistent with the XRD results. One possible explanation is that chalcopyrite and elemental sulfur were covered by jarosite, and only surface substances (<10 nm) can be detected by XPS.

Previous studies have demonstrated that the Ag-enhanced leaching of chalcopyrite was due to the formation of Ag_2S [31,36]. Table 2 shows that when bioleaching time increased from 5 to 23 days, the binding energy of S^{2-} shifted to the binding energy of Ag_2S [55], indicating that Ag–S bonds formed on the surface.

High-resolution spectra of Fe 2p are provided in Figure 7. Compared with chalcopyrite, the Fe 2p spectra show that the surface of bornite was heavily oxidized. The peak near 708 eV can be assigned to Fe−S [14]. The component near the binding energy of 712 eV can be assigned to jarosite. When bioleaching time increased from 5 to 30 days, the peak intensity of Fe−S decreased with increasing leaching time, while the peak intensity of jarosite increased with increasing leaching time (Figure 7). This is in agreement with Figure 6H. In other words, the mixed sample was bioleached when a mixed moderately thermophilic culture was employed.

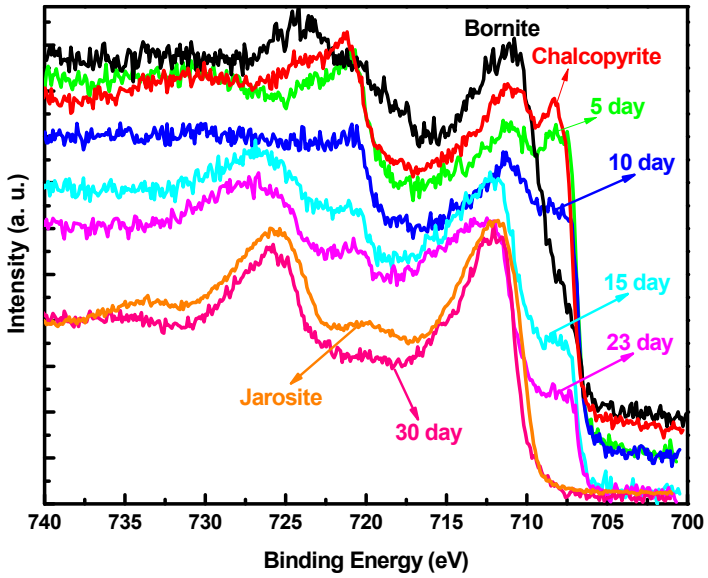

Figure 7. Fe 2p peaks of co-bioleaching chalcopyrite and bornite (ratio of Ccp/Bn was 3:1).

3.3. Electrochemical Behavior of Chalcopyrite and Bornite

The corrosion current density, corrosion potential and polarization resistance of chalcopyrite were 0.14 μA·cm^{-2}, 406.5 mV, and 165.2 kΩ·cm^2, respectively (Figure 8). Compared to chalcopyrite, the corrosion current density of bornite was greater, and the corrosion potential and polarization resistance of bornite were smaller. These values were 1.55 μA·cm^{-2}, 306.5 mV, and 23.9 kΩ·cm^2, respectively (Figure 8). The higher value of the corrosion current density or lower value of the polarization resistance means that the oxidation kinetics were higher during the dissolution process. On the other hand, when chalcopyrite and bornite were bioleached together, bornite dissolved preferentially compared to chalcopyrite due to the galvanic interactions because the open circuit potential (OCP) of bornite (340 mV) was lower than that of chalcopyrite (475 mV) (Figure 8). This is well in agreement with the leaching results.

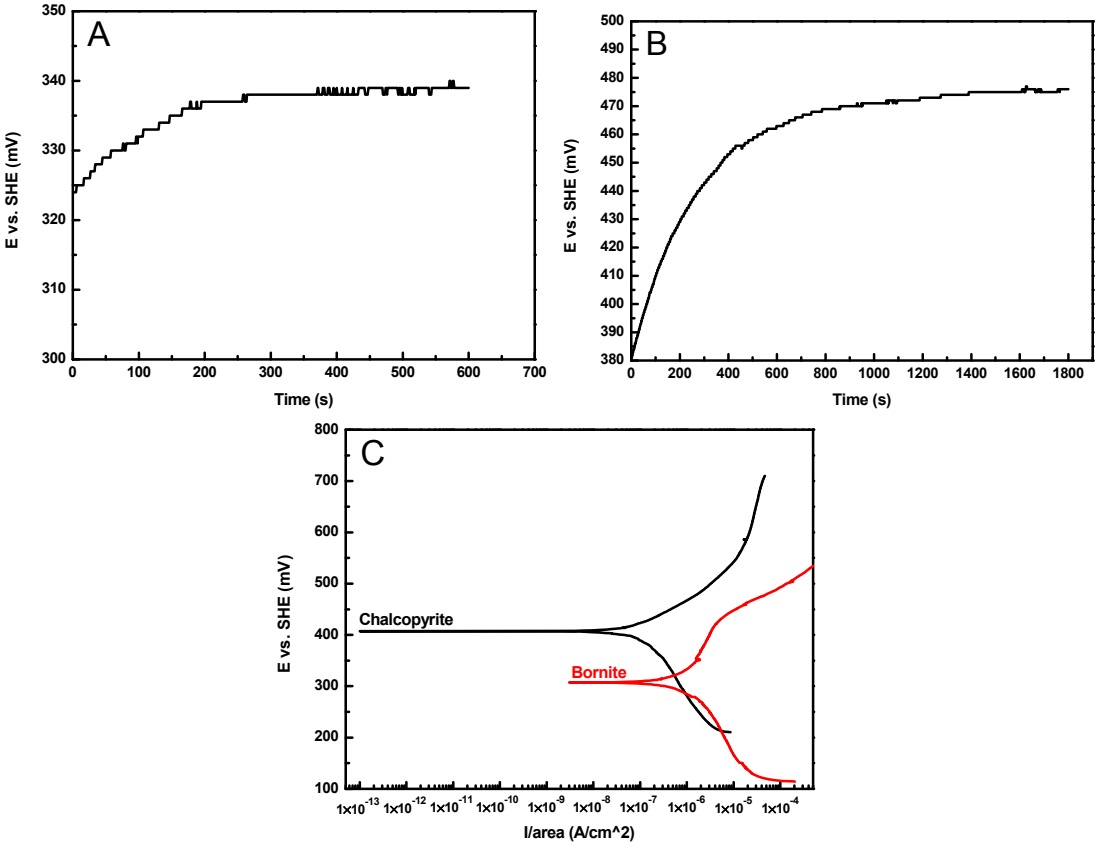

Figure 8. Open-circuit potential of massive bornite (**A**) and chalcopyrite (**B**) electrode. Tafel plot for chalcopyrite and bornite electrode (**C**).

4. Discussion

When silver-bearing bornite was dissolved preferentially due to the galvanic interactions, Ag^+ was also released into the solution. Ag^+ then diffused to the surface of chalcopyrite, and replaced Cu and Fe (Equation (1)) [36]. This resulted in the leaching of copper and iron from the chalcopyrite. Figures 3 and 5 show that silver accumulated onto the surface of the chalcopyrite, and Table 2 shows that the binding energy of S^{2-} shifted to the binding energy of Ag_2S. These findings agreed with previous studies that Ag_2S formed on the surface [31,36]. Ag^+ can be regenerated by oxidation of Ag_2S with Fe^{3+} (Equation (2)) [36]. Therefore, chalcopyrite can be continuously leached because it is silver-catalyzed. This result is well in agreement with previous studies [28,56]. On the other hand,

the OCP of Ag_2S was about 500 mV (vs. SHE) [57], and the contact between $CuFeS_2$ and Ag_2S could accelerate the dissolution of $CuFeS_2$ owing to the galvanic interactions:

$$CuFeS_2 + 4Ag^+ \rightarrow 2Ag_2S + Cu^{2+} + Fe^{2+} \quad (1)$$

$$Ag_2S + 2Fe^{3+} \rightarrow 2Ag^+ + 2Fe^{2+} + S^0 \quad (2)$$

S_2^{2-} and S_n^{2-} were detected on surface leaching residues during the bioleaching time from 5 to 23 days, but the Cu extraction percentage still increased from 46% to 84% (Figure 6H). In previous study, S_2^{2-} and S_n^{2-} were considered as chalcopyrite passive film [7,11,12]. However, higher Cu extraction has been obtained in the presence of Ag. Ghahremaninezhad et al. [37] proposed a new model for silver-catalyzed chalcopyrite leaching: when Ag^+ was present in solution, Ag^+ adsorbed onto the surface of the chalcopyrite passive film and formed Ag_2S; and the sulfur in Ag_2S was a sulfur vacancy. The sulfur vacancy caused a faster diffusion rate in passive film and the formation of a porous sulfur layer; thus, high Cu extraction has been obtained in the presence of Ag although S_2^{2-} and S_n^{2-} were detected on surface leaching residues during the bioleaching [37]. On the other hand, jarosite (SO_4^{2-}) and S^0 were detected during the leaching process, but the Cu extraction percentage increased with increased leaching time (Figure 6H). Many studies have indicated that neither jarosite nor S^0 hindered the dissolution of chalcopyrite [13,20,58,59].

5. Conclusions

The achieved results show that only 21.5% and 59.4% of Cu can be leached from chalcopyrite and silver-bearing bornite, respectively, using a mixed moderately thermophilic culture, while 94.6% of the Cu was successfully bioleached from the mixed sample (ratio of chalcopyrite/bornite was 3:1). Compared to bioleaching chalcopyrite or silver-bearing bornite alone, the Cu extraction percentage was greatly enhanced when they were co-bioleached. The results of XRD show that silver-bearing bornite dissolved preferentially compared to chalcopyrite, owing to the galvanic interactions. The Ag^+ released from silver-bearing bornite was enriched on the surface of the mineral, owing to the formation of Ag_2S. During the bioleaching process, Ag^+ can be regenerated by the oxidation of Ag_2S with Fe^{3+}; thus, chalcopyrite can be continuously leached when it is silver-catalyzed.

Acknowledgments: This work was supported by Provincial Science and Technology Leaders (Innovation team of interface chemistry of efficient and clean utilization of complex mineral resources, Grant No. 2016RS2016), the Co-Innovation Centre for Clean and Efficient Utilization of Strategic Metal Mineral Resources, and the Innovation Driven Plan of Central South University (Grant No. 2015CX005).

Author Contributions: C.Y. and W.Q. conceived and designed the experiments; C.Y. performed the experiments; C.Y. wrote the paper; and F.J. improved the paper.

Conflicts of Interest: The authors declare no conflict of interest.

References

1. Schlesinger, M.E.; King, M.J.; Sole, K.C.; Davenport, W.G. Chapter 1—Overview. In *Extractive Metallurgy of Copper*; Elsevier: Oxford, UK, 2011; pp. 1–12.
2. Wang, S. Copper leaching from chalcopyrite concentrates. *JOM* **2005**, *57*, 48–51. [CrossRef]
3. Panda, S.; Akcil, A.; Pradhan, N.; Deveci, H. Current scenario of chalcopyrite bioleaching: A review on the recent advances to its heap-leach technology. *Bioresour. Technol.* **2015**, *196*, 694–706. [CrossRef] [PubMed]
4. Watling, H.R. Chalcopyrite hydrometallurgy at atmospheric pressure: 2. Review of acidic chloride process options. *Hydrometallurgy* **2014**, *146*, 96–110. [CrossRef]
5. Watling, H.R. Chalcopyrite hydrometallurgy at atmospheric pressure: 1. Review of acidic sulfate, sulfate-chloride and sulfate-nitrate process options. *Hydrometallurgy* **2013**, *140*, 163–180. [CrossRef]
6. Li, Y.; Kawashima, N.; Li, J.; Chandra, A.P.; Gerson, A.R. A review of the structure, and fundamental mechanisms and kinetics of the leaching of chalcopyrite. *Adv. Colloid Interface Sci.* **2013**, *197*, 1–32. [CrossRef] [PubMed]

7. Wu, S.; Yang, C.; Qin, W.; Jiao, F.; Wang, J.; Zhang, Y. Sulfur composition on surface of chalcopyrite during its bioleaching at 50 °C. *Trans. Nonferrous Met. Soc. China* **2015**, *25*, 4110–4118. [CrossRef]
8. Córdoba, E.M.; Muñoz, J.A.; Blázquez, M.L.; González, F.; Ballester, A. Leaching of chalcopyrite with ferric ion. Part II: Effect of redox potential. *Hydrometallurgy* **2008**, *93*, 88–96. [CrossRef]
9. Córdoba, E.M.; Muñoz, J.A.; Blázquez, M.L.; González, F.; Ballester, A. Leaching of chalcopyrite with ferric ion. Part IV: The role of redox potential in the presence of mesophilic and thermophilic bacteria. *Hydrometallurgy* **2008**, *93*, 106–115. [CrossRef]
10. Zhao, H.; Huang, X.; Wang, J.; Li, Y.; Liao, R.; Wang, X.; Qiu, X.; Xiong, Y.; Qin, W.; Qiu, G. Comparison of bioleaching and dissolution process of p-type and n-type chalcopyrite. *Miner. Eng.* **2017**, *109*, 153–161. [CrossRef]
11. Klauber, C.; Parker, A.; van Bronswijk, W.; Watling, H. Sulphur speciation of leached chalcopyrite surfaces as determined by X-ray photoelectron spectroscopy. *Int. J. Miner. Process.* **2001**, *62*, 65–94. [CrossRef]
12. Mikhlin, Y.L.; Tomashevich, Y.V.; Asanov, I.P.; Okotrub, A.V.; Varnek, V.A.; Vyalikh, D.V. Spectroscopic and electrochemical characterization of the surface layers of chalcopyrite ($CuFeS_2$) reacted in acidic solutions. *Appl. Surf. Sci.* **2004**, *225*, 395–409. [CrossRef]
13. Majuste, D.; Ciminelli, V.S.T.; Osseo-Asare, K.; Dantas, M.S.S.; Magalhaes-Paniago, R. Electrochemical dissolution of chalcopyrite: Detection of bornite by synchrotron small angle X-ray diffraction and its correlation with the hindered dissolution process. *Hydrometallurgy* **2012**, *111*, 114–123. [CrossRef]
14. Ghahremaninezhad, A.; Dixon, D.G.; Asselin, E. Electrochemical and XPS analysis of chalcopyrite ($CuFeS_2$) dissolution in sulfuric acid solution. *Electrochim. Acta* **2013**, *87*, 97–112. [CrossRef]
15. Yin, Q.; Kelsall, G.H.; Vaughan, D.J.; England, K.E.R. Atmospheric and electrochemical oxidation of the surface of chalcopyrite ($CuFeS_2$). *Geochim. Cosmochim. Acta* **1995**, *59*, 1091–1100. [CrossRef]
16. He, H.; Xia, J.L.; Yang, Y.; Jiang, H.C.; Xiao, C.Q.; Zheng, L.; Ma, C.Y.; Zhao, Y.D.; Qiu, G.Z. Sulfur speciation on the surface of chalcopyrite leached by *Acidianus manzaensis*. *Hydrometallurgy* **2009**, *99*, 45–50. [CrossRef]
17. Crundwell, F.K. The semiconductor mechanism of dissolution and the pseudo-passivation of chalcopyrite. *Can. Metall. Q.* **2015**, *54*, 279–288. [CrossRef]
18. Vilcáez, J.; Suto, K.; Inoue, C. Bioleaching of chalcopyrite with thermophiles: Temperature–pH–ORP dependence. *Int. J. Miner. Process.* **2008**, *88*, 37–44. [CrossRef]
19. Yang, Y.; Liu, W.H.; Bhargava, S.K.; Zeng, W.M.; Chen, M. A XANES and XRD study of chalcopyrite bioleaching with pyrite. *Miner. Eng.* **2016**, *89*, 157–162. [CrossRef]
20. Qin, W.; Yang, C.; Lai, S.; Wang, J.; Liu, K.; Zhang, B. Bioleaching of chalcopyrite by moderately thermophilic microorganisms. *Bioresour. Technol.* **2013**, *129*, 200–208. [CrossRef] [PubMed]
21. Zhao, H.B.; Wang, J.; Gan, X.W.; Hu, M.H.; Tao, L.; Qin, W.Q.; Qiu, G.Z. Role of pyrite in sulfuric acid leaching of chalcopyrite: An elimination of polysulfide by controlling redox potential. *Hydrometallurgy* **2016**, *164*, 159–165. [CrossRef]
22. Zhao, H.; Wang, J.; Yang, C.; Hu, M.; Gan, X.; Tao, L.; Qin, W.; Qiu, G. Effect of redox potential on bioleaching of chalcopyrite by moderately thermophilic bacteria: An emphasis on solution compositions. *Hydrometallurgy* **2015**, *151*, 141–150. [CrossRef]
23. Yang, Y.; Liu, W.; Chen, M. XANES and XRD study of the effect of ferrous and ferric ions on chalcopyrite bioleaching at 30 °C and 48 °C. *Miner. Eng.* **2015**, *70*, 99–108. [CrossRef]
24. Sandström, Å.; Shchukarev, A.; Paul, J. XPS characterisation of chalcopyrite chemically and bio-leached at high and low redox potential. *Miner. Eng.* **2005**, *18*, 505–515. [CrossRef]
25. Hiroyoshi, N.; Hirota, M.; Hirajima, T.; Tsunekawa, M. A case of ferrous sulfate addition enhancing chalcopyrite leaching. *Hydrometallurgy* **1997**, *47*, 37–45. [CrossRef]
26. Berry, V.K.; Murr, L.E.; Hiskey, J.B. Galvanic interaction between chalcopyrite and pyrite during bacterial leaching of low-grade waste. *Hydrometallurgy* **1978**, *3*, 309–326. [CrossRef]
27. Mehta, A.P.; Murr, L.E. Fundamental studies of the contribution of galvanic interaction to acid-bacterial leaching of mixed metal sulfides. *Hydrometallurgy* **1983**, *9*, 235–256. [CrossRef]
28. Sato, H.; Nakazawa, H.; Kudo, Y. Effect of silver chloride on the bioleaching of chalcopyrite concentrate. *Int. J. Miner. Process.* **2000**, *59*, 17–24. [CrossRef]
29. Córdoba, E.M.; Muñoz, J.A.; Blázquez, M.L.; González, F.; Ballester, A. Leaching of chalcopyrite with ferric ion. Part III: Effect of redox potential on the silver-catalyzed process. *Hydrometallurgy* **2008**, *93*, 97–105. [CrossRef]

30. Gómez, E.; Ballester, A.; Blázquez, M.L.; González, F. Silver-catalysed bioleaching of a chalcopyrite concentrate with mixed cultures of moderately thermophilic microorganisms. *Hydrometallurgy* **1999**, *51*, 37–46. [CrossRef]
31. Miller, J.D.; Portillo, H.W. Silver catalysis in ferric sulfate leaching of chalcopyrite. In *Proceedings of the XIII International Mineral Processing Congress*; Elsevier Science: Warsaw, Poland, 1979; pp. 691–742.
32. Zhao, H.; Wang, J.; Gan, X.; Hu, M.; Zhang, E.; Qin, W.; Qiu, G. Cooperative bioleaching of chalcopyrite and silver-bearing tailing by mixed moderately thermophilic culture: An emphasis on the chalcopyrite dissolution with XPS and electrochemical analysis. *Miner. Eng.* **2015**, *81*, 29–39. [CrossRef]
33. Nikoloski, A.N.; O'Malley, G.P.; Bagas, S.J. The effect of silver on the acidic ferric sulfate leaching of primary copper sulfides under recycle solution conditions observed in heap leaching. Part 1: Kinetics and reaction mechanisms. *Hydrometallurgy* **2017**, *173*, 258–270. [CrossRef]
34. Nazari, G.; Dixon, D.G.; Dreisinger, D.B. The role of silver-enhanced pyrite in enhancing the electrical conductivity of sulfur product layer during chalcopyrite leaching in the Galvanox™ process. *Hydrometallurgy* **2012**, *113–114*, 177–184. [CrossRef]
35. Nazari, G.; Dixon, D.G.; Dreisinger, D.B. The mechanism of chalcopyrite leaching in the presence of silver-enhanced pyrite in the Galvanox™ process. *Hydrometallurgy* **2012**, *113*, 122–130. [CrossRef]
36. Miller, J.D.; McDonough, P.J.; Portillo, H.Q. Electrochemistry in silver catalysed ferric sulfate leaching of chalcopyrite. In *Process and Fundamental Considerations of Selected Hydrometallurgical Systems*; Kuhn, M.C., Ed.; Society of Mining Engineers: New York, NY, USA, 1981; pp. 327–338.
37. Ghahremaninezhad, A.; Radzinski, R.; Gheorghiu, T.; Dixon, D.G.; Asselin, E. A model for silver ion catalysis of chalcopyrite ($CuFeS_2$) dissolution. *Hydrometallurgy* **2015**, *155*, 95–104. [CrossRef]
38. Hiroyoshi, N.; Arai, M.; Miki, H.; Tsunekawa, M.; Hirajima, T. A new reaction model for the catalytic effect of silver ions on chalcopyrite leaching in sulfuric acid solutions. *Hydrometallurgy* **2002**, *63*, 257–267. [CrossRef]
39. Wang, J.; Qin, W.; Zhang, Y.; Yang, C.; Zhang, J.; Nai, S.; Shang, H.; Qiu, G. Bacterial leaching of chalcopyrite and bornite with native bioleaching microorganism. *Trans. Nonferrous Met. Soc. China* **2008**, *18*, 1468–1472. [CrossRef]
40. Wang, Y.-G.; Su, L.-J.; Zeng, W.-M.; Qiu, G.-Z.; Wan, L.-L.; Chen, X.-H.; Zhou, H.-B. Optimization of copper extraction for bioleaching of complex Cu-polymetallic concentrate by moderate thermophiles. *Trans. Nonferrous Met. Soc. China* **2014**, *24*, 1161–1170. [CrossRef]
41. Zhao, H.; Wang, J.; Hu, M.; Qin, W.; Zhang, Y.; Qiu, G. Synergistic bioleaching of chalcopyrite and bornite in the presence of *Acidithiobacillus ferrooxidans*. *Bioresour. Technol.* **2013**, *149*, 71–76. [CrossRef] [PubMed]
42. Bevilaqua, D.; Acciari, H.A.; Arena, F.A.; Benedetti, A.V.; Fugivara, C.S.; Tremiliosi, G.; Garcia, O. Utilization of electrochemical impedance spectroscopy for monitoring bornite (Cu_5FeS_4) oxidation by *Acidithiobacillus ferrooxidans*. *Miner. Eng.* **2009**, *22*, 254–262. [CrossRef]
43. Bevilaqua, D.; Garcia, O.; Tuovinen, O.H. Oxidative dissolution of bornite by *Acidithiobacillus ferrooxidans*. *Process Biochem.* **2010**, *45*, 101–106. [CrossRef]
44. Bevilaqua, D.; Diez-Perez, I.; Fugivara, C.S.; Sanz, F.; Garcia, O.; Benedetti, A.V. Characterization of bornite (Cu_5FeS_4) electrodes in the presence of the bacterium *Acidithiobacillus ferrooxidans*. *J. Braz. Chem. Soc.* **2003**, *14*, 637–644. [CrossRef]
45. Zhao, H.; Wang, J.; Gan, X.; Zheng, X.; Tao, L.; Hu, M.; Li, Y.; Qin, W.; Qiu, G. Effects of pyrite and bornite on bioleaching of two different types of chalcopyrite in the presence of Leptospirillum ferriphilum. *Bioresour. Technol.* **2015**, *194*, 28–35. [CrossRef] [PubMed]
46. Wang, J.; Tao, L.; Zhao, H.; Hu, M.; Zheng, X.; Peng, H.; Gan, X.; Xiao, W.; Cao, P.; Qin, W.; Qiu, G.; Wang, D. Cooperative effect of chalcopyrite and bornite interactions during bioleaching by mixed moderately thermophilic culture. *Miner. Eng.* **2016**, *95*, 116–123. [CrossRef]
47. Johnson, D.B.; Okibe, N.; Wakeman, K.; Yajie, L. Effect of temperature on the bioleaching of chalcopyrite concentrates containing different concentrations of silver. *Hydrometallurgy* **2008**, *94*, 42–47. [CrossRef]
48. Reich, M.; Palacios, C.; Barra, F.; Chryssoulis, S. "Invisible" silver in chalcopyrite and bornite from the Mantos Blancos Cu deposit, northern Chile. *Eur. J. Mineral.* **2013**, *25*, 453–460. [CrossRef]
49. Ying, L.; Wang, C.; Tang, J.; Wang, D.; Qu, W.; Li, C. Re–Os systematics of sulfides (chalcopyrite, bornite, pyrite and pyrrhotite) from the Jiama Cu–Mo deposit of Tibet, China. *J. Asian Earth Sci.* **2014**, *79*, 497–506. [CrossRef]

50. Yang, C.; Qin, W.; Lai, S.; Wang, J.; Zhang, Y.; Jiao, F.; Ren, L.; Zhuang, T.; Chang, Z. Bioleaching of a low grade nickel–copper–cobalt sulfide ore. *Hydrometallurgy* **2011**, *106*, 32–37. [CrossRef]
51. Yin, M.; Wu, C.K.; Lou, Y.B.; Burda, C.; Koberstein, J.T.; Zhu, Y.M.; O'Brien, S. Copper oxide nanocrystals. *J. Am. Chem. Soc.* **2005**, *127*, 9506–9511. [CrossRef] [PubMed]
52. Chusuei, C.C.; Brookshier, M.A.; Goodman, D.W. Correlation of relative X-ray photoelectron spectroscopy shake-up intensity with CuO particle size. *Langmuir* **1999**, *15*, 2806–2808. [CrossRef]
53. Goh, S.W.; Buckley, A.N.; Lamb, R.N.; Rosenberg, R.A.; Moran, D. The oxidation states of copper and iron in mineral sulfides, and the oxides formed on initial exposure of chalcopyrite and bornite to air. *Geochim. Cosmochim. Acta* **2006**, *70*, 2210–2228. [CrossRef]
54. Fuggle, J.C.; Källne, E.; Watson, L.M.; Fabian, D.J. Electronic structure of aluminum and aluminum-noble-metal alloys studied by soft-X-ray and X-ray photoelectron spectroscopies. *Phys. Rev. B* **1977**, *16*, 750–761. [CrossRef]
55. Kaushik, V.K. XPS core level spectra and Auger parameters for some silver compounds. *J. Electron Spectrosc. Relat. Phenom.* **1991**, *56*, 273–277. [CrossRef]
56. Hu, Y.; Qiu, G.; Wang, J.; Wang, D. The effect of silver-bearing catalysts on bioleaching of chalcopyrite. *Hydrometallurgy* **2002**, *64*, 81–88. [CrossRef]
57. Córdoba, E.M.; Muñoz, J.A.; Blázquez, M.L.; González, F.; Ballester, A. Comparative kinetic study of the silver-catalyzed chalcopyrite leaching at 35 and 68 °C. *Int. J. Miner. Process.* **2009**, *92*, 137–143. [CrossRef]
58. D'Hugues, P.; Foucher, S.; Galle-Cavalloni, P.; Morin, D. Continuous bioleaching of chalcopyrite using a novel extremely thermophilic mixed culture. *Int. J. Miner. Process.* **2002**, *66*, 107–119. [CrossRef]
59. Gu, G.; Hu, K.; Zhang, X.; Xiong, X.; Yang, H. The stepwise dissolution of chalcopyrite bioleached by *Leptospirillum ferriphilum*. *Electrochim. Acta* **2013**, *103*, 50–57. [CrossRef]